G&G Lab Notes

Editors
Thomas M. Moses | Shane F. McClure

DIAMOND

Large Artificially Irradiated Yellow

Natural diamonds that have been laboratory-irradiated to obtain a more desirable color are quite common today. Recently the New York laboratory examined a 50.86 ct emerald-cut diamond with a Fancy Vivid yellow color (figure 1), a desirable grade that would fetch a high price in the market—provided the color was natural.

The diamond was very clean, receiving a clarity grade of VVS_2. It was evenly colored and had no apparent color zoning, though a very weak brown graining was observed with diffuse lighting. Initial gemological observations did not seem to indicate irradiation, but spectroscopic data proved otherwise.

Figure 1. Spectroscopic analysis showed that this 50.86 ct Fancy Vivid yellow emerald-cut diamond had been artificially irradiated.

UV-visible absorption spectroscopy showed a "cape" spectrum common for this color of diamond. Mid-infrared absorption spectroscopy proved it was a type Ia diamond, but also revealed very weak bands at ~5165 and 4935 cm^{-1} (H1c and H1b), which aroused some concern as to the origin of color. Using a custom-made high-resolution UV-Vis spectrometer, we detected a very weak absorption peak at ~595 nm, indicative of artificial radiation treatment in this type of diamond (G.R. Crowningshield, "Spectroscopic recognition of yellow bombarded diamonds," Winter 1957–58 *G&G*, pp. 99–104, 117). Also observed was strong absorption at ~503 nm (H3), the center responsible for the yellow color. The brown graining suggested that the stone originally had a brown color and underwent irradiation and subsequent annealing to achieve the Fancy Vivid yellow appearance.

The successful treatment of this stone resulted in a color found in large natural-color diamonds, such as a 127 ct cape diamond from the Kimberley mine in South Africa that was also recently graded by GIA.

GIA's laboratory frequently encounters artificially irradiated diamonds, but they are usually much smaller. GIA previously graded this 50.86 ct diamond in 1992 and identified it as treated. It remains one of the largest artificially irradiated diamonds seen in the laboratory.

Paul Johnson

Editors' note: All items were written by staff members of GIA laboratories.

Gems & Gemology, Vol. 48, No. 2, pp. 132–141, http://dx.doi.org/10.5741/GEMS.48.2.132.

Multi-Treated Yellowish Green

While radiation-induced defects are commonly responsible for green color in diamond, either artificially or by natural processes, the color is often not very saturated. Recently examined in the Carlsbad laboratory was a 0.99 ct diamond (figure 2) with a Fancy Deep yellowish green color that resulted from a multistep process involving irradiation and HPHT treatments. Multi-treatment processing has been documented for orange, pink, and red

Figure 2. This 0.99 ct diamond's saturated yellowish green color resulted from a multistep process involving HPHT treatment and irradiation.

diamonds (see, e.g., W. Wang et al., "Treated-color pink-to-red diamonds from Lucent Diamonds Inc.," Spring 2005 *G&G*, pp. 6–19; and Winter 2005 Lab Notes, pp. 341–342), but only recently has GIA seen multi-treated saturated green diamonds.

Microscopic examination of the yellowish green diamond revealed brown graining and an etched cleavage. Strong green emission was observed with fiber-optic illumination, indicating the presence of the H3 defect. When examined in immersion, the diamond displayed a subtle green zone near the culet.

The FTIR absorption spectrum revealed that this was a type Ia diamond with resolvable A- and B-aggregated nitrogen impurities, hydrogen-related defects, and nitrogen-aggregate platelets. The FTIR spectrum also showed evidence of both HPHT treatment and post-HPHT irradiation; H1a defects (1450 cm^{-1}) resulting from irradiation were particularly prominent. UV-Vis-NIR spectroscopy showed absorption features at 595, 666, and 741 (GR1) nm, confirming that artificial irradiation had imparted a significant green color component.

Because of the observed brown graining and the indications of treatment, we infer that this stone started as a brown type Ia diamond that was HPHT-treated to a saturated yellow to greenish yellow color. Next, artificial irradiation was used to intensify the green component, creating an unusually saturated color. This type of product could fill the market gap for highly saturated green diamonds.

Nathan Renfro and Christopher M. Breeding

Natural Green, Artificially Irradiated for Color Enhancement

Some gem diamonds are naturally irradiated, giving rise to very rare blue to green hues. Laboratory irradiation with a high-energy beam is one common form of diamond treatment used to induce a blue to green color. The New York laboratory recently encountered an intense green diamond that originally had a naturally light green color which was enhanced by artificial irradiation.

Figure 3. This 0.83 ct cushion-cut diamond was color graded as Fancy Intense green. Its naturally light yellow-green color had been enhanced by artificial irradiation.

This 0.83 ct cushion cut (5.64 × 5.59 × 3.16 mm) was color graded as Fancy Intense green (figure 3). The color was evenly distributed. It was identified as a type Ia diamond with a high concentration of aggregated nitrogen and weak hydrogen-related absorption. UV-Vis spectroscopy showed a strong GR1 absorption (zero-phonon line at 741.2 nm), as well as weak 594 nm, weak H3 (ZPL at 503.2 nm), and moderate N3 (ZPL at 415.3 nm) absorptions. Records revealed that this stone had been tested previously by GIA's laboratory, but was color graded as Light yellow-green. Gemological and spectroscopic features at that time confirmed that it was a natural diamond and attributed the green color to natural irradiation and related GR1 absorptions. In the resubmitted Fancy Intense green diamond, however, the absorption intensity of GR1 had nearly doubled (using N3 intensity as an internal reference, which should remain stable). Based on this, we believe that the color improvement from light yellow-green to intense green was due to artificial irradiation. This conclusion was also supported by other spectroscopic data.

Naturally and artificially irradiated diamonds share many gemological and spectroscopic features. When a naturally light blue to green diamond is irradiated to enhance its color saturation, this can be very difficult to detect. Successful identification of this diamond was achieved through extensive spectroscopic analysis and careful documentation of its grading history.

Wuyi Wang, Siau Fung Yeung, and Ivana Kayes

Pink Diamonds with 478 nm Peak

Pink diamonds are rare in nature and command a high price accordingly. They can be either type IIa (with no detectable nitrogen) or type Ia (nitrogen-bearing). A broad band at ~550 nm observed in the visible absorption spectrum is usually responsible for the pink color. A typical type IaAB pink diamond—from the Argyle mine, for example—shows a characteristic visible spectrum with absorptions at 415 nm (N3) and 496/530 nm (H3), in addition to the broad band at ~550 nm. Other causes of pink coloration include concentrations of pink color in glide planes (type IaA diamonds) and occasionally nitrogen-vacancy (N-V) centers.

The New York laboratory examined three natural pink brilliants with unusual spectral features: a 0.35 ct Fancy Light pink pear, a 1.16 ct Fancy Light pink cushion, and a 0.80 ct Faint pink round (figure 4). These diamonds were submitted at different times starting in mid-2010. All were type Ia, but their UV-Vis spectra showed an absorption at 478 nm, a peak attributed to the N2 optical center typically seen in the spectra of yellow "cape" diamonds. The presence of a cape spectrum and an absorption at ~550 nm raised our suspicions of a coating. Although GIA has identified many coated pinks with this type of spectrum, these three brilliants showed no evidence of coating, and pink graining was visible throughout each stone (figure 5). We concluded that these were natural-color pink diamonds with very rare spectral features often attributed to cape diamonds.

Figure 4. These three natural-color pink diamonds showed a UV-Vis absorption peak at 478 nm, a feature normally associated with yellow "cape" diamonds. From left to right, they consist of a 0.35 ct Fancy Light pink, a 1.16 ct Fancy Light pink, and a 0.80 ct Faint pink.

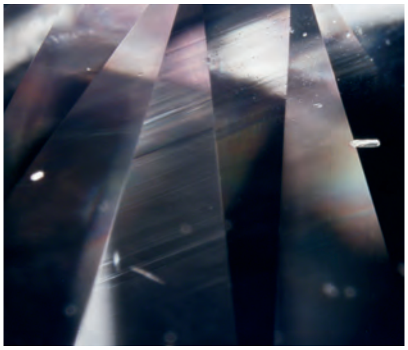

Figure 5. Pink graining is visible through the pavilion facets of the 0.80 ct round brilliant. Magnified 50×.

The 550 nm absorption band, which is responsible for pink coloration in many natural diamonds, may occur with varying aggregations and concentrations of nitrogen. As these diamonds show, there is not necessarily any correlation between the formation of this optical center and the natural aggregation process of nitrogen in diamond.

Marzena Nazz and Paul Johnson

Rough Diamonds with a Green Coating

Faceted diamonds, both colorless and fancy-color, are sometimes surface-coated to improve their color appearance. In the New York laboratory, we recently encountered two rough diamonds that had been coated green.

Submitted for color origin testing, the two crystals (figure 6) showed rounded octahedral shapes and weighed 15.77 ct (14.83 × 9.76 × 14.54 mm) and 14.42 ct (12.18 × 11.37 × 13.74 mm). Under the microscope, they displayed a green surface-related coloration with uneven distribution (figure 7), similar to the appearance of naturally colored rough diamonds with strong green radiation stains. Yet the coatings were easily detected because the green color was restricted to the surface, rather than penetrating slightly into the crystal. In addition, the coating on the 14.42 ct crystal had partially worn off, revealing the underlying yellow bodycolor. When they were scratched with a pointer probe, the coating easily came off.

These coated rough diamonds serve as a reminder that some of the older, simpler treatments never go away, so it is always important to look for them. An unsuspecting buyer could easily be fooled by the general appearance of these crystals.

Emiko Yazawa

Figure 6. These rough diamond crystals (15.77 and 14.42 ct) were coated to mimic the appearance of naturally irradiated green diamonds.

Figure 7. A closer view of this diamond crystal (magnified 20×) shows the uneven distribution of the strong green surface coloration.

Jewelry Mounted with Red FELDSPAR from China

Two fine orangy red gems mounted in jewelry were recently submitted to the New York laboratory for identification. One specimen was a modified cushion cut measuring 14.70 × 10.90 × 7.75 mm, and the other was a modified heart measuring 16.85 × 15.30 × 9.10 mm (figure 8). The stones had refractive indices of 1.557–1.567 and were inert to long- and short-wave UV radiation, properties that identified them as feldspar. Specific gravity could not be measured because of the mountings, so their identity was confirmed using Raman spectroscopy. Microscopic examination of the cushion cut revealed bands of fine particles and short aligned needles, dotted with small reflective platelets. The heart shape showed general turbidity in fiber-optic lighting, but had no discrete inclusions.

Figure 8. These two orangy red gems (left—10.90 mm wide, and right—15.30 mm wide) were identified as plagioclase (andesine-labradorite). The origin of their color—natural or induced by copper diffusion—could not be determined.

Despite the economic importance of red feldspar in some markets, particularly in Asia, we rarely see this material submitted to the laboratory for identification. This is quite interesting, given the controversy over the color origin of red feldspar from certain deposits (see, e.g., A. Abduriyim et al., "Research on gem feldspar from the Shigatse region of Tibet," Summer 2011 *G&G*, pp. 167–180). The natural color of material from Oregon is generally undisputed, although treated samples have been seen. These samples are easily distinguishable, however, by their unusually high copper concentrations or atypical inclusion scenes. With Chinese material, there is no practical means of identifying whether the color is natural or induced by copper diffusion.

Using quantitative chemical analysis, it is possible to distinguish red feldspar from different localities (see figure 9, and also G. R. Rossman, "The Chinese red feldspar controversy: Chronology of research through July 2009," Spring 2011 *G&G*, pp. 16–30). Therefore, it is also possible to establish whether the color of a red feldspar is natural, as is the case for most material from Oregon, or undetermined, as with Inner Mongolian and Tibetan material. LA-ICP-MS analyses of the two samples yielded chemical compositions of $An_{48.9}Ab_{47.8}Or_{3.3}$ and $An_{51.0}Ab_{46.0}Or_{3.0}$, which correlate well with andesine-labradorite from China. Copper was detected in both samples. In light of their Chinese origin, we could not be certain that their color was natural. For their identification reports, we followed the lab's policy in stating that "color origin cannot currently be determined."

Emily V. Dubinsky and Ren Lu

Figure 9. The chemical compositions of gem-quality plagioclase from various localities, determined by quantitative LA-ICP-MS analysis, are clearly separated in this ternary plot. The compositions of the two red feldspars described in this study, shown as red squares, are consistent with material from China.

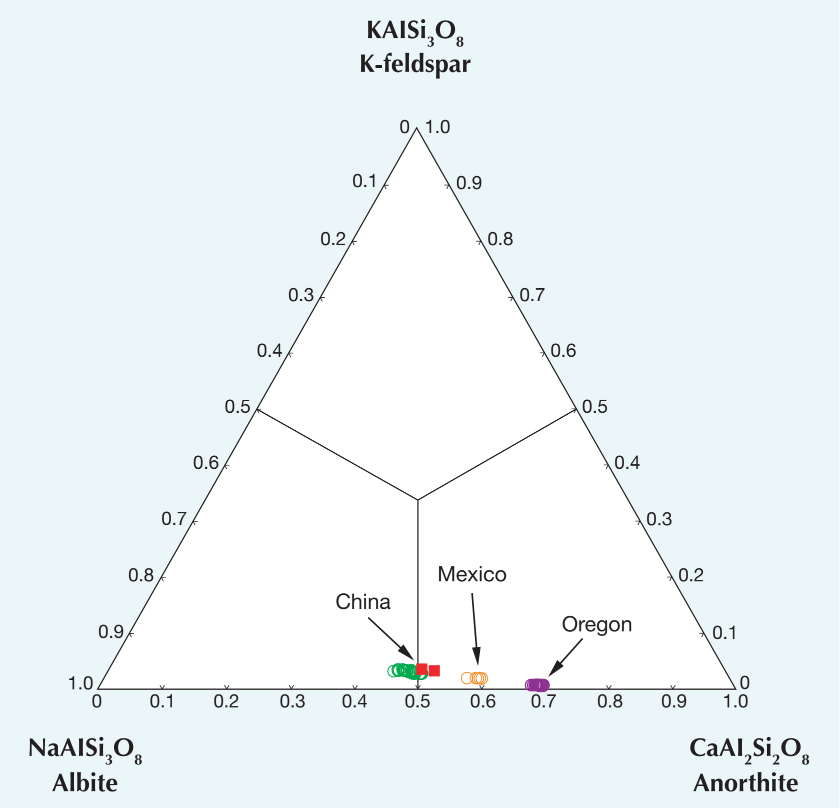

HIBONITE Crystal

Recently examined at the Carlsbad laboratory was a 3.1 g partially polished hexagonal crystal (figure 10) that proved to be a very rare collector mineral.

Initial microscopic observations revealed stepped etch features and numerous fractures and cleavages throughout. The sample contained dark brown mineral inclusions and some negative crystals, but their contents were not resolvable through the rough surface. A partially polished surface gave a spot RI of 1.79, though it was a vague reading as the polish was rather poor, and the hydrostatic SG was 3.80. Raman analysis revealed prominent features at 900 and 872 cm^{-1}, but the spectra did not match any samples in GIA's reference database.

The crystal's color and morphology were similar to those of hibonite specimens reportedly from Myanmar (T. Hainschwang et al., "Hibonite: A new gem mineral," Summer 2010 *G&G*, pp. 135–138). To confirm the identity, quantitative chemical data collected with LA-ICP-MS and its Raman spectrum were very consistent with those reported by Hainschwang et al. While the crystal we examined was much larger, only very small areas were clean enough to potentially yield faceted stones.

This was the first example of hibonite examined at the Carlsbad laboratory, and it illustrates the importance of familiarity with the gemological literature. Because of the increasingly specialized nature of gemology, a literature search may be the only resource to help identify an unusual gem material.

Nathan Renfro

Figure 10. This 3.1 g crystal was identified as the rare mineral hibonite.

Unusual Green Color in a JADEITE Bangle

The Carlsbad laboratory recently examined a jadeite bangle that showed an unusual band of green color (figure 11). While mottled white jade with irregular green patches or zones of color is not uncommon, these colored areas are usually due to naturally occurring chromium or artificially introduced green dye.

A spectroscope is useful for differentiating the cause of green color in jadeite; both chromium and dye show distinctive features in the red region of the spectrum. However, when this bangle was examined with a spectroscope, neither feature was observable in the red region, suggesting that the green color was not caused by either chromium or dye.

Under magnification the piece displayed a natural fibrous to granular structure. The green color followed a finer and denser zone that crosscut the bangle. This textural anomaly had the appearance of an irregular shear zone that occurred in the jadeite rock during its formation, causing a localized change in structure. All of the mineral grains, including those in the irregularly textured zone, appeared tightly interlocked and showed no indications of repair or manufacture.

Figure 11. This 58.3 g (70.70 × 12.93 mm) polymer-impregnated jadeite bangle showed a prominent green band caused by an optical flash effect.

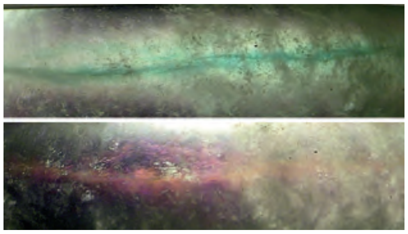

Figure 12. The impregnated bangle showed a green flash in brightfield lighting (top) and an orange flash in darkfield conditions (bottom). This color variation confirmed that a flash effect—not dye or chromium—was the cause of the bangle's green color band.

The green color proved to be due to a vivid flash effect that was visible when the observer's line of sight was nearly parallel to the textured zone against a light background (figure 12, top). When the same part of the bangle was examined against a black background, the flash effect displayed an orange color (figure 12, bottom). This color variation between brightfield and darkfield conditions proves that the green color was an optical effect, and not caused by dye or traces of natural chromium in the jadeite. With FTIR spectroscopy, polymer impregnation was confirmed by the presence of a strong absorption band centered around 3000 cm^{-1} that completely saturated the detector of the instrument.

While a flash effect due to polymer impregnation in jadeite has been previously reported (Spring 2010 Lab Notes, pp. 54–55), this was the first time the lab had seen a prominent green color caused by the flash effect. The fact that this effect strongly resembled the green color expected in jadeite added to the intrigue of this bangle.

Nathan Renfro

Greenish Blue Imitation OPAL

The Carlsbad laboratory recently examined a semitransparent, vibrant greenish blue 6.89 ct modified oval brilliant (figure 13) similar to material being sold as synthetic opal under the trade name "PeruBlu."

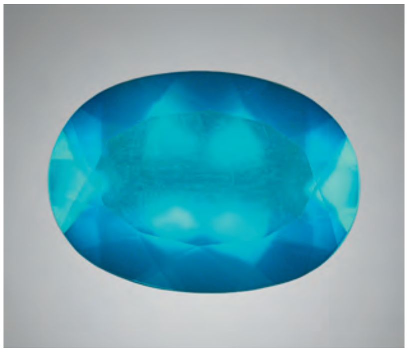

Figure 13. This 6.89 ct greenish blue modified oval brilliant is an imitation opal.

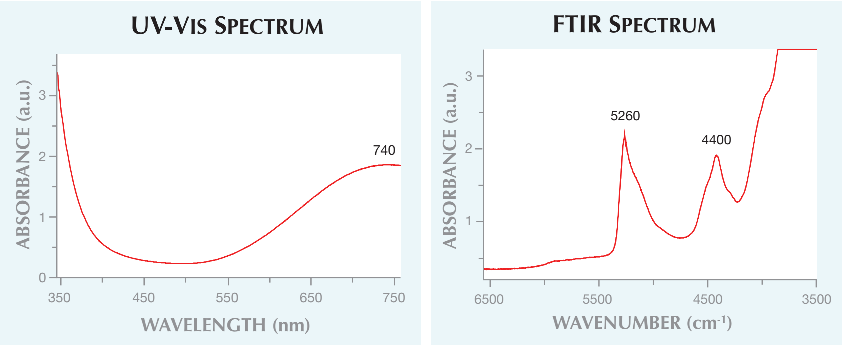

Figure 15. The UV-Vis absorption spectrum of the imitation opal shows broad absorption centered at 740 nm and a large transmission window at ~500 nm (left). Prominent features at ~5260 and 4400 cm^{-1} are seen in the IR spectrum (right).

While the sample appeared generally clean under low magnification, a closer look with a standard gemological microscope revealed wispy clouds and an artificial-looking, fine-grained, granular appearance that is not common to natural opal and caused a hazy quality. Pinpoint inclusions with faint optical halos (figure 14) were scattered throughout the sample. It had an RI of 1.339, with an additional faint shadow edge at 1.350, indicating the material might be composed of multiple components. The very low RI quickly ruled out natural opal. The hydrostatic SG of 1.54 was also well below the range expected for natural opal. In cross-polarized light, the sample displayed strong anomalous double refraction as prominent "snake bands." It was inert to long- and short-wave UV radiation.

Figure 14. Microscopic examination of the imitation opal with shadowed illumination showed a granular pattern and small pinpoint inclusions surrounded by an optical halo. Image width 0.80 mm.

UV-Vis spectroscopy revealed a strong absorption band centered at 740 nm and general absorption in the UV region, leaving a large transmission window centered at approximately 500 nm (figure 15, left). This spectrum was consistent with the observed greenish blue color. In addition to Si, EDXRF qualitative chemical analysis detected significant amounts of Cu along with very minor amounts of K and Cl. It is likely that the greenish blue color is caused by copper absorption. Since many Cu-colored minerals display a greenish blue color, the presence of Cu in this sample was not surprising.

Raman spectroscopy produced a featureless trace, consistent with an amorphous material. FTIR spectroscopy (figure 15, right) revealed prominent absorption features at ~5260 and ~4400 cm^{-1}. These absorptions are quite similar to those seen in the early version of MexiFire synthetic opal (G. Choudhary and R. Bhandari, "A new type of synthetic fire opal: Mexifire," Fall 2008 *G&G*, pp. 228–233). Except for its color, the appearance and the low RI and SG properties were also consistent with those reported for the MexiFire product, which has much different gemological properties than natural Peruvian opal (e.g., Winter 2003 GNI, p. 332).

Because the RI and SG values fell below any published values for natural common opal (e.g., R. Webster and P. G. Read, *Gems: Their Sources, Description, and Identification*, 5th ed., Butterworth-Heinemann, Oxford, UK, 2002), it is the lab's opinion that this sample is more properly described as an imitation, rather than a synthetic. This marked the first time the Carlsbad laboratory has encountered this material, even though a similar product has been available since 2007 (A. Abduriyim and T. Kobayashi, "Synthetic opal called 'MexiFire' and 'PeruBlu,'" *Gemmology*, Vol. 39, No. 464, 2008, pp. 2–3).

Nathan Renfro and Amy Cooper

PEARL

Cultured Freshwater Pearl Necklace Resembling Natural Saltwater Pearls

Recently, the New York laboratory received what appeared to be a typical antique-style pearl necklace with a small gold fishhook clasp. The knotted 20-inch (50.8 cm) necklace was comprised of graduated near-round to semibaroque white cultured pearls (3.38–7.08 mm; figure 16, left). The lab receives numerous pieces like this each month, and the overwhelming majority of the specimens prove to be natural saltwater pearls from mollusks of the *Pinctada* genus (e.g., figure 16, right). The rest are generally bead-cul-

Figure 16. The necklace on the left, composed of non-bead cultured freshwater pearls (3.38–7.08 mm), resembles a typical natural saltwater pearl necklace (see example on the right; 3.40–5.25 mm).

tured saltwater pearls or a mixture of these and natural saltwater pearls.

This necklace caught our attention when most of the cultured pearls' micro X-radiographs displayed dark linear irregular central features typical of the growth structures in freshwater non-bead cultured pearls (figure 17). The EDXRF spectrum and strong white fluorescence to X-rays revealed noticeable traces of manganese, confirming a freshwater origin. Despite all outward appearances, this necklace was composed of non-bead cultured freshwater pearls.

In many ways this piece was atypical of white freshwater cultured pearl strands, which tend to have a neutral white color and uniform size and shape, typically button, oval, or semi-baroque (figure 18). The present necklace was created using rounder graduated cultured pearls of a creamier color on a knotted string—all very typical of natural saltwater strands. In fact, the lab has begun to see freshwater pieces apparently intended to imitate older natural saltwater strands, either through their assembly or through physical modification of the cultured pearls to make them appear old and worn.

The last few years have seen increasing demand for natural saltwater pearls. Most consumers and many dealers in the jewelry industry have little experience with natural saltwater pearls due to their rarity and high cost. Items such as this necklace are a reminder to take extra caution when dealing with apparent natural saltwater pearl strands, since their cultured freshwater counterparts occupy the opposite end of the value spectrum.

Chunhui Zhou and Akira Hyatt

Large Freshwater Cultured Blister Pearl

The practice of culturing blister pearls dates back to ancient China, where small lead images of Buddha were placed inside the shells of freshwater mussels. Today blister pearls are cultured in various types of mollusks. Blister pearls also form naturally and can be quite large, such as a 97.80 ct sample examined by GIA's Bangkok laboratory (N. Sturman, "A large naturally colored natural blister pearl," GIA News from Research, www.gia.edu/research-resources/news-from-research/index.html, June 10, 2009).

A very large cultured blister pearl (figure 19) was recently submitted to the New York laboratory for identification. The baroque-shaped cream-colored specimen measured approximately 60.58 × 56.64 × 26.80 mm and weighed 517 ct. One side of it was fairly flat and displayed severed growth rings (figure 20), clear evidence of having been cut away from the shell, while the other side was nacreous and exhibited noticeable orient.

In addition to its extraordinary size, this cultured blister pearl had an-

Figure 17. X-radiographs of the client's necklace revealed the linear growth structure typical of non-bead cultured freshwater pearls (left, ~5 mm in diameter) rather than the concentric growth structure found in natural saltwater pearls (right, ~4 mm each).

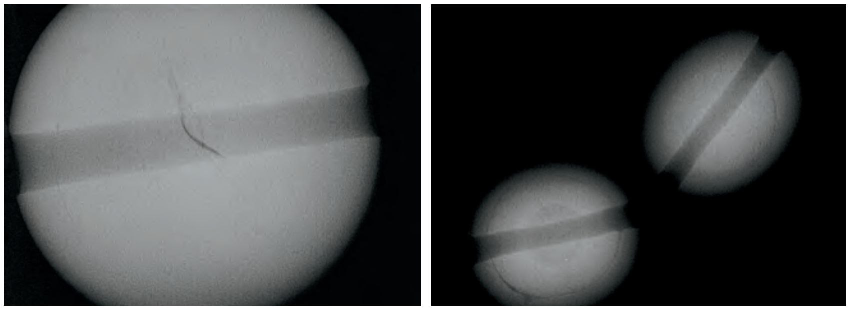

Figure 18. Most non-bead cultured freshwater pearl strands (here, with a maximum diameter of 3.60–4.50 mm) have a neutral white color and uniform size and shape.

Figure 19. This massive freshwater cultured blister pearl (shown with a 13 mm South Sea cultured pearl for comparison) weighs 517 ct and measures 60.58 × 56.64 × 26.80 mm.

other unusual feature: At least 10 distinct small cultured pearls were embedded in it, visible on the side where it had been cut from the shell (again, see figure 20). Within each one, X-radiography revealed the growth structures typical of nonbead-cultured freshwater pearls (e.g., figure 21).

The sample's strong yellow fluorescence to X-rays and EDXRF spectrum confirmed that it had a freshwater origin, in that it contained noticeable traces of manganese. A considerable amount of lead was also found in various parts of the blister's surface, which is not typical of either freshwater or saltwater pearls. Bioaccumulation in a polluted water environment can contribute to heavy metal concentrations in mollusk shells and tissues (S. K. Gupta and J. Singh, "Evaluation of mollusc as a sensitive indicator of heavy metal pollution in aquatic system [*sic*]: A review," *The IIOAB Journal,* Vol. 2, No. 1, 2011, pp. 49–57).

The unusual aggregate structure suggested that the large cultured blister pearl may have resulted from normal culturing gone awry. Typically, multiple freshwater pearls are cultured in a single mussel at one time. In this case, it appears that the secretion of nacre had grown out of control for some reason—possibly the result of the lead contamination—engulfing the small individual cultured pearls.

Although this is not the first freshwater cultured blister pearl we have seen, its large size, unusual structure, and anomalous lead content make it a unique and interesting specimen.

Chunhui Zhou and Akira Hyatt

Figure 20. A close-up view of the sawn flat side of the cultured blister pearl reveals numerous embedded small cultured pearls. Image width ~26 mm.

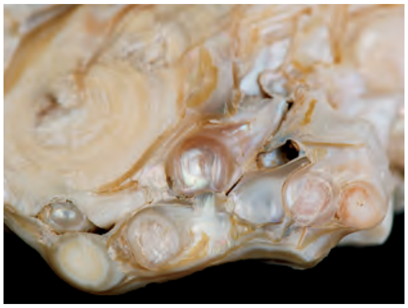

Figure 21. This X-radiograph image shows the outlines of some of the small nonbead-cultured pearls in the specimen. Image width ~16 mm.

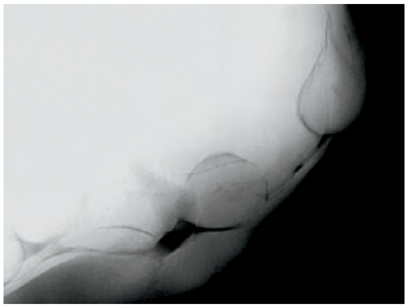

Luminescent STRONTIUM-CALCIUM ALUMINATE Doped with Rare-Earth Elements

In January 2012 the New York laboratory received for identification two unusual manufactured products, submitted within one week of each other. One was a yellowish green decorative vessel (figure 22) carved in the style of Asian jade or serpentine, with detailed patterns in relief; it measured approximately 20.20 × 8.00 × 7.50 cm and weighed 583.20 g. The other was a yellowish green and orangy brown piece of "rough" measuring approximately 11.0 × 7.2 × 6.7 mm and weighing 0.89 g (figure 23).

The carved vessel gave a spot RI of 1.65, and the rough piece's hydrostatic SG was 3.48; neither displayed any features in the desk-model spectroscope. Both showed a very strong yellowish green fluorescence to long- and short-wave UV radiation, and a strong green phosphorescence that lasted for more than 10 minutes. The same phosphorescence reaction was achieved using a strong fiber-optic light and in a light box using daylight-equivalent 6500 K bulbs. Microscopic examination of both samples revealed a uniform, granular texture with tiny, evenly distributed hexagonal grains and a pitted surface. Some dark brown stains were observed along fractures. LA-ICP-MS analysis showed that both pieces had essentially the same chemical composition, with major amounts of Sr, Al,

Figure 22. This 583.20 g carved vessel, composed of strontium-calcium aluminate doped with rare-earth elements, displayed a strong green phosphorescence reaction, as shown on the right.

and Ca, as well as minor amounts of Eu, Dy, and B. Raman spectroscopy also recorded similar features for both, with a main peak at 464 cm^{-1} and several minor peaks. Additional LA-ICP-MS data and the full Raman spectra are available in the *G&G* Data Depository at www.gia.edu/gandg.

Figure 23. This 0.89 g piece of strontium-calcium aluminate showed the same phosphorescence reaction as the carving in figure 22.

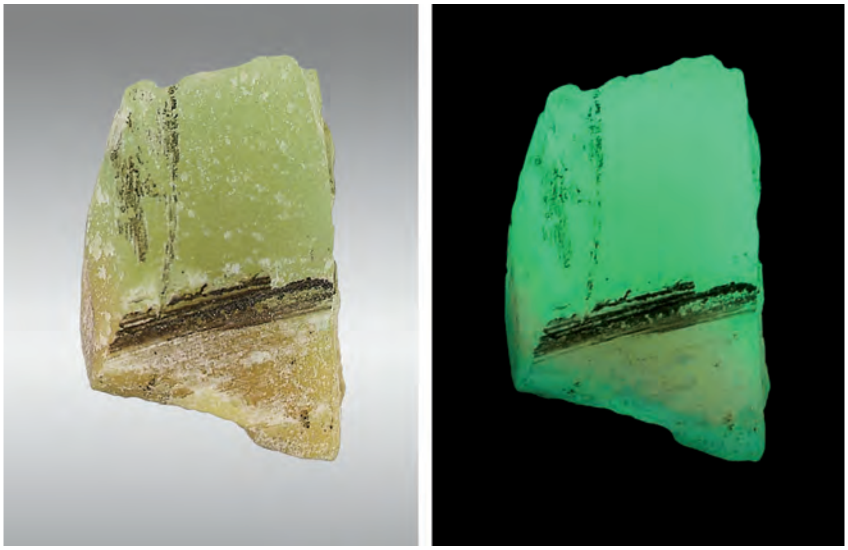

Many of these properties were consistent with a manufactured product represented at the 2002 Tucson gem show as "Nightglow Stone" (Winter 2002 Gem News International, pp. 358–360), which consisted of strontium aluminate doped with Eu^{2+} and Dy^{3+} to produce a very strong green phosphorescence. That material was reportedly produced by a sintering method, and the granular appearance of these two pieces was consistent with such a preparation. In 2005, a "night glowing pearl" coated with a similar material was also submitted to GIA for an identification report (see Spring 2005 Lab Notes, pp. 46–47), demonstrating a persistent interest in producing glowing gem materials.

Rare earth–doped strontium aluminate phosphors hold promise for the development of long-lasting phosphorescence applications, an important area of research. Chemical variations in the strontium aluminate host, as well as the type of activator, have yielded different afterglow colors and intensities. Various preparation techniques have been used, often with the addition of B_2O_3, which is regarded as an excellent flux to facilitate the diffusion process and reduce the synthesis temperature (Y.-L. Chang et al., "Characterizations of Eu, Dy co-doped $SrAl_2O_4$ phosphors prepared by the solid-state reaction with B_2O_3 addition," *Journal of Alloys and Compounds*, Vol. 461, 2008, pp. 598–603). The sintering temperature and the particle size of the phosphor also play important roles in determining the luminescence quality of the material (S. Hamdan et al., "Morphology and composition of strontium calcium aluminate matrix doped with Dy^{3+}," *Materials Science and Technology*, Vol. 27, No. 1, 2011, pp. 232–234).

Luminescent materials have many practical applications, such as emergency signage and alternative lighting sources. They are also being used to make interesting decorative objects.

Claire Ito

Figure 24. This 0.50 ct HPHT-grown synthetic diamond (left) was produced by AOTC. DiamondView images display strong blue to green fluorescence (middle) and intense blue phosphorescence (right). The middle image clearly shows the cuboctahedral growth pattern typical of HPHT-grown synthetic diamonds.

Near-Colorless HPHT-Grown SYNTHETIC DIAMONDS from Advanced Optical Technology Co.

Manufacturers of HPHT-grown synthetic diamonds have generally focused on fancy colors due to the ease of incorporating color-inducing impurities along with the faster growth rates that result in larger polished products. The majority of colorless to near-colorless HPHT synthetic specimens have been grown solely for research purposes by companies such as General Electric, De Beers, and Sumitomo Electric Industries. Near-colorless HPHT synthetics, though very rare, have also been marketed to the gem trade by Advanced Optical Technology Co. (AOTC).

Recently, three near-colorless and three faintly colored HPHT-grown AOTC synthetic diamonds were submitted to GIA's New York laboratory for grading services. These products can be purchased through AOTC's trade-only website or through their consumer-oriented brand, D.NEA, and each synthetic bears the inscription "AOTC-created." The diamonds are said to be manufactured using BARS- or toroid-type presses. AOTC also loaned us 24 colorless, near-colorless, and faintly and lightly colored HPHT-grown synthetic diamonds.

All 30 of the samples were faceted as round brilliants, ranging from 0.21 to 0.57 ct (e.g., figure 24, left). Most received colorless to near-colorless grades, with six classified as F and 17 falling in the G–J range. The remaining seven were very faint to light blue. Clarities ranged from VVS$_1$ to I$_2$, with no correlation between the color and clarity grades. The poorer clarities resulted from elongated opaque or metallic flux-metal inclusions. Graining was not evident, and only subdued interference colors (gray/blue), characteristic of HPHT synthetics, were observed.

Infrared absorption spectroscopy revealed that they were mixed type IIa/IIb, with only traces of boron detected. Nitrogen and boron impurities in diamond produce yellow and blue colors, respectively. It is the careful balance between the relative concentrations of these two impurities, at low concentrations, that gave rise to the near-colorless appearance of most of the samples. Although color zoning was not noticeable, the growth sector–dependent impurity uptake was obvious in DiamondView fluorescence images (e.g., figure 24, center). The samples exhibited strong blue to green fluorescence and intense, long-lived (1–6 minutes) blue phosphorescence (figure 24, right). This behavior differed from that seen using a standard UV lamp. The samples were inert to long-wave (366 nm) radiation, but showed very faint to strong yellow fluorescence to short-wave (254 nm) excitation. In the latter case, we observed strong greenish yellow phosphorescence with a persistent blue component.

Photoluminescence (PL) spectroscopy revealed that no one emission peak was characteristic of all the synthetic diamonds. Nitrogen vacancies (575.0 and 637.0 nm) and a peak at 658 nm were observed in some samples, independent of the press-type used. The latter peak has been reported in nickel-containing HPHT-grown synthetic diamonds, but was here noted in samples attributed to Ni-free toroid press production. An additional group of three peaks at 706.9, 709.1, and 712.2 nm was usually detected in the samples containing 658 nm peaks. The defect(s) responsible for these peaks have not been established. Nickel-related emissions (484 and 882.6/884.3 nm doublet) were identified in most of the BARS-grown synthetics. Nickel impurities, often observed in HPHT synthetic diamonds grown using Ni catalysts, are rare in natural diamonds. A weak H3 center (503.2 nm) was detected in three of the samples. One specimen (toroid press production, I color, I$_2$ clarity) did not show distinctive PL features.

This line of HPHT-grown synthetics can be confidently identified by careful analysis of data from a combination of advanced testing techniques, especially fluorescence imaging and PL spectroscopy.

Ulrika F. S. D'Haenens-Johansson, Kyaw Soe Moe, Paul Johnson, Shun Yan Wong, and Wuyi Wang

PHOTO CREDITS:

Jian Xin (Jae) Liao—1, 3–6, 8, 16, 18–20, 22–24 (left); Robison McMurtry—2, 11, 12; Jason Darley—7; C. D. Mengason—10, 13; Nathan Renfro—14; Chunhui Zhou—17, 21; Sood-Oil (Judy) Chia—22, 23; Jian Xin (Jae) Liao—24 (left) Kyaw Soe Moe—24 (center and right).